applied sciences

MDPI

Article

A Statistical Procedure for Analyzing the Behavior of Air Pollutants during Temperature Extreme Events: The Case Study of Emilia-Romagna Region (Northern Italy)

Maria Ragosta [1,*], Mariagrazia D'Emilio [2], Luciana Casaletto [1] and Vito Telesca [1]

[1] Engineering School, University of Basilicata, 85100 Potenza, Italy; luciana.casaletto83@gmail.com (L.C.); vito.telesca@unibas.it (V.T.)
[2] Consiglio Nazionale delle Ricerche Institute of Methodologies for Environmental Analysis, Tito Scalo, 85050 Potenza, Italy; mariagrazia.demilio@imaa.cnr.it
* Correspondence: maria.ragosta@unibas.it

Featured Application: The characterization of the correlation structure among air pollutants during heat waves may be useful for decision makers that have the responsibility of taking additional measures to prevent health effects on the population when extreme temperatures are forecasted.

Abstract: Meteorological conditions play a crucial role in air pollution by affecting both directly and indirectly the emissions, transport, formation, and deposition of air pollutants. Extreme weather events can strongly affect surface air quality. Understanding relations between air pollutant concentrations and extreme weather events is a fundamental step toward improving the knowledge of how excessive heat impacts on air quality. In this work, we developed a statistical procedure for investigating the variations in the correlation structure of four air pollutants (NO_x, O_3, PM_{10}, $PM_{2.5}$) during extreme temperature events measured in monitoring sites located of Emilia Romagna region, Northern Italy, in summer (June–August) from 2015 to 2017. For the selected stations, Hot Days (HDs) and Heat Waves (HWs) were identified with respect to historical series of maximum temperature measured for a 30-year period (1971–2000). This method, based on multivariate techniques, allowed us to highlight the variations in air quality of study area due to the occurrence of HWs. The examined data, including PM concentrations, show higher values, whereas NO_x and O_3 concentrations seem to be not influenced by HWs. This operative procedure can be easily exported in other geographical areas for studying effects of climate change on a local scale.

Keywords: local climate variability; air pollution; multivariate statistics

check for updates

Citation: Ragosta, M.; D'Emilio, M.; Casaletto, L.; Telesca, V. A Statistical Procedure for Analyzing the Behavior of Air Pollutants during Temperature Extreme Events: The Case Study of Emilia-Romagna Region (Northern Italy). *Appl. Sci.* **2021**, *11*, 8266. https://doi.org/10.3390/app11178266

Academic Editor: Francisco Barraza

Received: 30 July 2021
Accepted: 3 September 2021
Published: 6 September 2021

Publisher's Note: MDPI stays neutral with regard to jurisdictional claims in published maps and institutional affiliations.

Copyright: © 2021 by the authors. Licensee MDPI, Basel, Switzerland. This article is an open access article distributed under the terms and conditions of the Creative Commons Attribution (CC BY) license (https://creativecommons.org/licenses/by/4.0/).

1. Introduction

In the last years, the scientific research linked to human health and wellbeing of populations in urban and industrialized areas mainly focused on two issues: climate change and air quality [1–10]. Climate change affects human wellbeing through many related events: increased frequency and intensity of heat waves and cold waves, changing precipitation intensity, and increased devastating weather events, such as hurricanes, tornadoes, floods and droughts, cold-related mortality, and heat-related mortality [11–17]. Observed climate trends show that temperatures are increasing, particularly extreme temperatures, with heat waves (HWs) becoming more frequent, more intense, and longer lasting [3,17–20]. In literature, many studies are focused on the effects of HWs and air pollution on human health, particularly on the increase in mortality and morbidity, whilst few studies investigate the link between HWs and air pollution [2,21–24].

Climate change is intrinsically connected to air pollution because the main driver of climate change is fossil fuel combustion, which is also a major contributor to air pollution. In

fact, combustion processes emit both greenhouse gases (CO_2, CH_4, N_2O) and air pollutants (PM, SO_2, NO_x, CO) [25–28]. Meteorological conditions seem to influence atmospheric concentrations of ozone, particulate matter, and nitrogen oxides. These air pollutants are a major threat to human health; particularly, they are dangerous for older people, people with heart disease, and children. Inadequate pollutant dispersion due to topographic and meteorological conditions, such as low wind intensity, cause the stagnation of the chemical air mass, associated with peak pollution episodes [29–31].

We focused our investigation on Po plain, an area in which many studies have shown a strong influence of dispersion conditions for all particle matter ranges, a distinct anthropogenic periodicity (seasonal and diurnal) for many pollutants, and a strong dependence on atmospheric conditions. Our study analyses data collected during the summers of the years 2015–2017 in the Emilia Romagna Region (Italy). We focus on this region because of its severe urban air pollution due to the high population and industrial manufacturing density and to the fact of being in a valley where two surrounding mountain chains favor the stagnation of pollutants [29–31]. Extreme temperature events (Hot Days and Heat Waves) in selected 14 regional stations were identified with respect to a 30-year period (1971–2000). The objective of this study was to develop an operative procedure based on multivariate techniques for investigating the relationship between temperature and air quality during Hot Days and Heat Waves and for evaluating the impact of temperature on air pollutant concentrations.

2. Materials and Methods

2.1. Study Area

The study was carried out in Emilia Romagna (Figure 1), a region of Northern Italy that largely includes the Po Valley, delimited by Tusco-Emilian Apennines to the south, with mountains reaching altitude of 2000 m.a.s.l. A climate gradient, from the Mediterranean warm-temperate climate to the cold-temperate climate of the Apennines, is present in the region. In the Po plain, summers are hot, winters are cold (typical monthly mean temperatures ranging from 1 °C to 26 °C), and autumns rainy. This region is characterized by high humidity levels (typical monthly mean relative humidity ranging from 60% to 84%) and low wind intensities (typical annual mean wind intensities of about 2 m/s). The Emilia Romagna region is densely populated and suffers a strong anthropic pressure due to urban areas, heavy industrialization, and intensive breeding and agriculture.

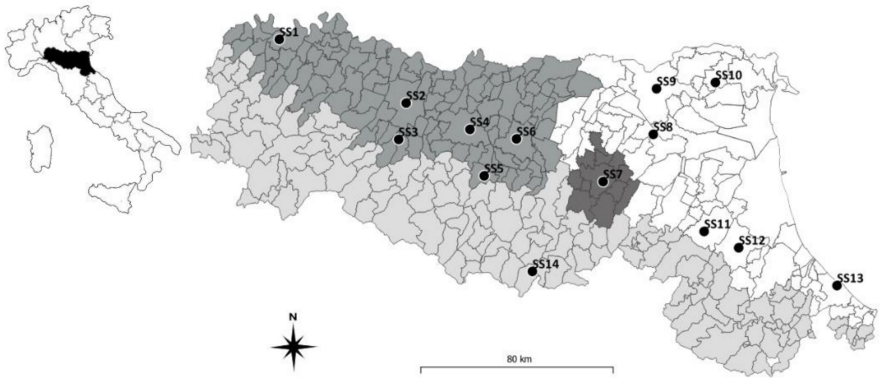

Figure 1. Study area and sampling sites. In light grey: Apennine mountains and hill area; in dark grey: west plain area; in white: east plain area; in black: the agglomeration area (Bologna city) (www.arpae.it) accessed on 1 July2021.

2.2. Data

In this work, 14 sampling sites (SS) were selected. The sampling points are located either in rural areas or in background urban or suburban areas. Moreover, the stations are representative of the four areas in which the territory of the region is classified, the agglomeration area of Bologna city and the three different geographical zones: west plain

area, east plain area, and Apennine mountains and hill area (Figure 1). Each sampling site consists of an air-quality monitoring station and a closer meteorological station managed by the Regional Agency for Prevention, Environment, and Energy of Emilia-Romagna (www.arpae.it accessed on 1 July 2021). The sampling sites are listed in Table 1. For each site, we analyze the following six descriptors (DSs), reduced at daily scale and collected during summer (1 June–31 August) from 2015 to 2017: PM_{10} daily concentrations ($\mu g/m^3$):

- $PM_{2.5}$ daily concentrations ($\mu g/m^3$);
- NO_x daily concentrations ($\mu g/m^3$);
- O_3 daily concentrations ($\mu g/m^3$);
- T_{max} daily maximum temperature (°C); and
- RH_{min} daily minimum relative humidity (%).

Table 1. Sampling sites: in the last two columns, the classification according to Air Quality Monitoring Network of Emilia-Romagna region (AQ cl.) and the altitude (Q).

Label		Geographical Zone	Municipality	AQ cl.	Q (m.a.s.l.)
SS1	Montecucco	West plain area	Piacenza	Urban	61
SS2	Cittadella	West plain area	Parma	Urban	60
SS3	Badia	Westplain area	Parma	Rural	202
SS4	San Lazzaro	West plain area	Reggio Emilia	Urban	55
SS5	Castellarano	West plain area	Reggio Emilia	Suburban	150
SS6	Parco Ferrari	West plain area	Modena	Urban	30
SS7	G. Margherita	Bologna area	Bologna	Urban	43
SS8	S.Pietro Capofiume	Eastplain area	Bologna	Rural	11
SS9	Villa Fulvia	East plainarea	Ferrara	Urban	8
SS10	J. di Savoia	East plain area	Ferrara	Rural	−2
SS11	Parco Bertozzi	Eastplain area	Ravenna	Urban	35
SS12	Parco Resistenza	Eastplain area	Forlì-Cesena	Urban	29
SS13	Marecchia	East plain area	Rimini	Urban	5
SS14	Porretta Terme	Apennine mountains and hill area	Bologna	Rural	970

For each sampling site, we used historical series of maximum temperatures for the reference 30-year period (1971–2000); we selected this reference period on the base of the suggestion given by WMO (World Meteorological Organization) to update CLINO every ten years [32,33]. The entire database was checked to guarantee the goodness of fit and to avoid the presence of anomalies; to this aim, ad-hoc routines were implemented in R environment for automatically detecting missing data. In all the examined data, the percentage of data missing is less than 5%; in the other cases, the data are considered not available.

2.3. Data Analysis Procedure

Using historical series of maximum temperature and following the methodology proposed in [3], Hot Days (HD) and Heat Waves (HW) for each sampling site and for each summer were determined. For each station, we defined the degree of severity of these extreme events, comparing the 2015–2017 data with the respective historical time series from 1971–2000. The current daily value of temperature was compared with its mean historical value, including standard deviation (σ). We define Hot Days of the first degree HD_{L1} if the current value is higher than historical values $\pm\sigma$; Hot Days of the second degree HD_{L2} with $n\{HD_{L2}\} \leq n\{HD_{L1}\}$, if the current value is higher than historical values $\pm 2\sigma$; and Hot Days of the third degree HD_{L3} with $n(HD_{L3}) \leq n\{HD_{L2}\} \leq n\{HD_{L1}\}$, if the current value is higher than historical values $\pm 3\sigma$. Furthermore, to measure the persistence of these events, the occurrence of Heat Waves is defined with the following criteria: occurrence of at least six consecutive days classified as HD_{L1} = occurrence of Heat Wave of the first degree HW_{L1}; occurrence of at least six consecutive days classified as HD_{L2} = occurrence

of Heat Wave of the second degree HW_{L2}; and occurrence of at least six consecutive days classified as HD_{L3} = occurrence of Heat Wave of the third degree HW_{L3}.

In a second step, multivariate statistical procedures were applied [34,35]. For each sampling site, all data related to summer 2015–2017 were organized in data matrices at daily scale. Cluster Analysis (CA) and Principal Component Analysis (PCA) were applied to highlight the underlying correlation structure between pollutants concentrations and meteorological parameters [36]. CA is a classification technique used for determining homogeneous subgroups of sampling sites. For each data matrix, we calculated the association matrix using the Euclidean distance, and we applied the clustering algorithm at complete linkage. For results validation, each cluster has to be characterized by means of endogenous indices (centroids are the mean values of descriptors measured in SS included in the cluster) and by means of exogenous indices (mean values of variables external to the clustering procedure). The correspondence among endogenous and exogenous indices allowed us to explain the clustering structure. If the data matrix is correctly constructed, the results must not depend on the selected parameters

PCA is the most common factorial technique for reducing the space dimensionality and for highlighting the underlying correlation structure among measured variables. For determining the principal components (PCs), starting from data matrices, we calculated the eigenvalues and the corresponding eigenvectors of correlation matrix (association matrix based on Pearson coefficient). The eigenvectors represent the mutually orthogonal linear combinations of the original descriptors, and each of them can be considered a new independent variable. In order to investigate the nature of the new variables, or PC, we analyzed the percentage loadings matrix in which each element represents the percentage weight of the original descriptor in the PC.

For highlighting differences in the correlation structures among pollutants and meteorological parameters, we used Hot Days and Heat Waves identification procedure for selecting specific subsets of sampling days. We introduced two external variables with double modalities: (HD/noHD) and (HW/noHW). On the base of value assumed by bimodal variables, the original data matrices, including all the summer days $M_{SS}^{y} = [m \times n]$ (in which SS indicates the sampling site, y the year, m the number of sampling days $m \leq 92$, and n the number of descriptors), may be divided in the following submatrices:

1 HD-Submatrix $(M_{HD})_{SS}^{y} = [m_{HD} \times n]$ and noHD-Submatrix $(M_{noHD})_{SS}^{y} = [m_{noHD} \times n]$, for which $(M_{HD})_{SS}^{y} \cup (M_{noHD})_{SS}^{y} = M_{SS}^{y}$ with $m_{HD} \leq m$. Basically, we divided the original matrix into two submatrices one containing only HD days and the other containing only non-HD days; and

2 HW-Submatrix $(M_{HW})_{SS}^{y} = [m_{HW} \times n]$ and noHW-Submatrix $(M_{noHW})_{SS}^{y} = [m_{noHW} \times n]$, for which $(M_{HW})_{SS}^{y} \cup (M_{noHW})_{SS}^{y} = M_{SS}^{y}$ with $m_{HW} \leq m_{HD} \leq m$. Additionally, in this case, we divided the original matrix in two parts: the first that contains only the days that fall within a defined interval HW and another that contains only the days that do not belong to intervals of HW.

This procedure may be repeated also introducing the degree of severity for HD and HW, reducing the number of sampling days included in the submatrices, and increasing the level of risk. For all these different submatrices, PCA is applied in order to characterize the different correlation structures.

3. Results and Discussion

3.1. HD and HW Characterization

Hot Days and Heat Waves of the three levels of severity identified for the 14 study sites are shown in Tables 2 and 3. We highlight that the three threshold series used to identify extreme events were obtained using historical temperature series proper for each site station; in this way, the extreme event occurrences were identified with a higher degree of accuracy because linked to strictly local information.

Table 2. Hot Days (in parenthesis, in italic, the percentage calculated in summer, 92 sampling days). Legend: $n(HD_{L1})$ = number of Hot Days of the first level; $n(HD_{L2})$ = number of Hot Days of the second level; $n(HD_{L3})$ = number of Hot Days of the third level.

	2015			2016			2017		
	$n(HD_{L1})$	$n(HD_{L2})$	$n(HD_{L3})$	$n(HD_{L1})$	$n(HD_{L2})$	$n(HD_{L3})$	$n(HD_{L1})$	$n(HD_{L2})$	$n(HD_{L3})$
SS1	40 (*43%*)	9 (*10%*)	0	14 (*15%*)	1 (*1%*)	0	35(*38%*)	5 (*5%*)	0
SS2	39 (*42%*)	12 (*13%*)	2 (*2%*)	17 (*18%*)	1 (*1%*)	0	38 (*41%*)	13 (*14%*)	0
SS3	59 (*64%*)	19 (*20%*)	3 (*3%*)	36 (*39%*)	6 (*6%*)	0	57 (*62%*)	21 (*22%*)	3 (*3%*)
SS4	45 (*49%*)	9 (*10%*)	0	9 (*10%*)	0	0	38 (*41%*)	12 (*13%*)	0
SS5	50 (*54%*)	12 (*13%*)	0	29 (*31%*)	4 (*4%*)	0	55 (*60%*)	17 (*18%*)	3 (*3%*)
SS6	52 (*56%*)	17 (*18%*)	3 (*3%*)	27 (*29%*)	4 (*4%*)	0	54 (*58%*)	20 (*21%*)	4 (*4%*)
SS7	31 (*33%*)	4 (*4%*)	0	9 (*10%*)	0	0	30 (*32%*)	5 (*5%*)	0
SS8	37 (*40%*)	9 (*10%*)	0	13 (*14%*)	2 (*2%*)	0	38 (*41%*)	7 (*7%*)	0
SS9	34 (*37%*)	12 (*13%*)	0	16 (*17%*)	2 (*2%*)	0	39 (*42%*)	9 (*10%*)	1 (*1%*)
SS10	40 (*43%*)	13 (*14%*)	2 (*2%*)	15 (*16%*)	3 (*3%*)	0	36 (*39%*)	7 (*7%*)	1 (*1%*)
SS11	47 (*51%*)	14 (*15%*)	1 (*1%*)	28 (*30%*)	4 (*4%*)	0	49 (*53%*)	16 (*17%*)	1 (*1%*)
SS12	40 (*43%*)	12 (*13%*)	0	20 (*22%*)	3 (*3%*)	0	41 (*44%*)	14 (*15%*)	1 (*1%*)
SS13	38 (*41%*)	8 (*9%*)	1 (*1%*)	18 (*19%*)	1 (*1%*)	0	34 (*37%*)	10 (*11%*)	1 (*1%*)
SS14	36 (*39%*)	3 (*3%*)	0	13 (*14%*)	0	0	36 (*39%*)	9 (*10%*)	0

Table 3. Heat Waves (in parenthesis, the length of each HW expressed in days). Legend: $n(HW_{L1})$ = number of Heat Waves of the first level; $n(HW_{L2})$ = number of Heat Waves of the second level.

	2015		2016	2017
	$n(HW_{L1})$	$n(HW_{L2})$	$n(HW_{L1})$	$n(HW_{L1})$
SS1	3 (7,8,12)			2 (6,7)
SS2	3 (7,13,6)			2 (6,7)
SS3	5 (8,6,8,15,6)	1 (9)	2 (6,7)	5 (8,7,9,7,8)
SS4	4 (8,8,14,6)			4 (7,7,6,7)
SS5	4(8,12,14,6)			6 (8,7,8,7,8,8)
SS6	4 (8,8,14,6)	1 (8)		6 (8,7,8,7,8,8)
SS7	1 (8)			1 (6)
SS8	2 (8,8)			5 (6,6,6,7,7)
SS9	2 (6,9)	1 (7)		3 (6,6,7)
SS10	3 (7,6,10)	1 (8)		4 (6,6,7,6)
SS11	2 (8,10)	1 (8)	1 (6)	5 (6,7,7,6,7)
SS12	2 (7,10)			3 (6,7,6)
SS13	2 (7,10)			
SS14	3 (6,8,10)			4(8,6,7,6)

From Table 2, we note that 2015 and 2017 present higher events of HD_{L1}, HD_{L2}, and HD_{L3} respect to 2016; Table 3 shows that we record HW_{L1} for all the stations (except for SS13 during 2017) in 2015 and 2017, while only three HW_{L1} are recorded in 2016 for SS3 and SS11 stations. HW_{L2} are observed in 2015 in few stations (SS3, SS6, SS9, SS10, SS11), whereas no heat wave of the third level is recorded.

Comparing these results with those obtained in an area of Southern Italy (Matera, Basilicata) during summer 2015–2017, we note that, using the same method, the number of HDs and HWs highlighted in the second case are greater. Particularly, we note the marked presence of second- and third-level HWs, which instead are rare in Emilia-Romagna. This is probably due to the difference between the two examined regions: in Emilia-Romagna, the anthropogenic pressure of the last 40 years has remained unchanged, while in Matera, there has been a significant variation in land use [3,11].

3.2. Cluster Analysis on 2015–2017 Data

In Table 4, mean values of all the six descriptors are shown. If we focus on pollution data, we note that the recorded values, the maximum values included, do not exceed the alarm threshold stated by Italian law, which incorporates the European indications [37]. If we compare the values measured in the selected sampling sites with the data shown in the literature for similar studies, we note that they are low, both those measured by Mavrakys et al. [24] and those measured by Kalisa et al. [2]

Table 4. Mean values of pollutants concentrations, maximum daily temperature (T_{max}), and minimum daily relative humidity (RH_{min}) measured in 2015; 92 sampling days (n.a., not available data).

2015	**PM_{10}**	**$PM_{2.5}$**	**NO_x**	**O_3**	**T_{max}**	**RH_{min}**
	($\mu g/m^3$)	**($\mu g/m^3$)**	**($\mu g/m^3$)**	**($\mu g/m^3$)**	**(°C)**	**(%)**
SS1	25.6	17.5	15.8	88.8	31.4	30.3
SS2	26.1	14.4	13.3	98.3	31.8	33.1
SS3	21.0	12.9	6.6	104.4	31.5	32.3
SS4	20.4	13.6	13.0	83.8	32.4	28.75
SS5	19.4	12.5	9.4	98.2	31.0	n.a.
SS6	20.2	13.4	17.7	81.9	31.9	28.4
SS7	19.6	12.6	16.0	88.1	31.4	27.8
SS8	20.6	12.5	9.6	73.0	32.0	34.0
SS9	20.8	11.8	10.8	80.9	31.2	33.1
SS10	24.6	16.7	8.1	86.9	30.7	n.a.
SS11	n.a.	n.a.	n.a.	n.a.	n.a.	n.a.
SS12	17.7	10.0	16.5	86.2	31.0	30.9
SS13	23.4	14.1	17.4	86.2	28.7	40.1
SS14	14.1	9.4	3.8	86.8	29.3	n.a.
2016	**PM_{10}**	**$PM_{2.5}$**	**NO_x**	**O_3**	**T_{max}**	**RH_{min}**
SS1	14.3	19.6	16.4	78.5	30.1	30.9
SS2	20.8	11.2	13.6	89.3	30.4	33.4
SS3	16.1	9.3	7.2	90.8	30.2	32.2
SS4	17.2	11.0	14.8	73.6	31.4	31.6
SS5	16.3	10.2	7.9	89.1	29.6	n.a.
SS6	16.8	10.0	19.4	79.3	30.3	30.5
SS7	15.4	9.7	14.3	84.3	29.7	29.9
SS8	15.9	9.6	4.9	67.2	30.2	37.8
SS9	16.7	8.1	10.0	80.1	29.6	35.7
SS10	18.5	12.3	6.3	77.4	28.5	n.a.
SS11	14.6	8.2	8.6	79.6	31.1	33.3
SS12	13.9	7.6	7.9	77.4	29.3	33.6
SS13	18.3	9.7	15.7	77.4	27.3	41.8
SS14	10.8	6.2	2.3	61.0	27.6	n.a.
2017	**PM_{10}**	**$PM_{2.5}$**	**NO_x**	**O_3**	**T_{max}**	**RH_{min}**
SS1	15.5	21.8	13.3	85.9	31.8	n.a.
SS2	23.5	11.4	12.7	94.5	32.4	28.5
SS3	18.1	9.6	6.6	106.5	32.1	26.4
SS4	18.8	11.2	13.8	83.6	33	24.7
SS5	20.1	11.2	10.8	100.8	31.8	n.a.
SS6	19.9	9.8	18.5	87.2	32.4	24.8
SS7	16.8	10.4	10.8	94.6	31.9	24.9
SS8	18.8	10.1	6.4	60.8	32.3	32.3
SS9	18.9	8.5	8.5	85.3	31.7	31.3
SS10	20.4	12.6	8.3	78.7	30.5	n.a.
SS11	17.0	9.3	10.2	84.3	33.3	26.6
SS12	16.3	9.3	11.4	91.3	31.5	29.6
SS13	21.8	10.2	16.6	91.3	28.9	34.4
SS14	14.5	7.7	1.8	82.2	30.1	n.a.

To put in evidence homogeneous subgroups of sampling sites, in our statistical procedure, we applied a clustering algorithm. We repeated the clustering procedure twice, the first time taking into account all pollutants and meteorological parameters available and the second time eliminating RH_{min} because, as shown in Table 4, it presents a great deal of data missing. We obtained similar results so, for brevity, here, we show only the results of the procedure applied eliminating RH_{min}. For each year, data matrices are M_{2015} = *[13 SS × 5 DS]*; M_{2016} = *[14 SS × 5 DS]*; and M_{2017} = *[14 SS × 5 DS]*.

The dendrograms (Figure 2) show that SS2 Cittadella, SS3 Badia, and SS5 Castellarano have a high level of similarity during all the examined periods. These three stations, from a geographical point of view, are located in the west plain area and have a high on sea level of 60 m.a.s.l., 202 m.a.s.l., and 150 m.a.s.l., respectively. All of them are characterized by low concentrations of NO_x and high values of O_3. In 2015 and 2016, SS8 San Pietro Capofiume and SS14 Porretta Terme showed isolated elements in the dendrograms. They are located in two different geographical areas: the east plain area and Apennine Mountain area; have

two different highs on sea level (11 m.a.s.l. and 970 m.a.s.l.); and are characterized by very low pollutants concentrations.

3.3. Combined Analysis of HD/HW Occurrence and Pollutants Concentrations

In the groups SS2, SS3, and SS5, highlighted by cluster procedure, the frequency of Hot Days is higher than in the other SSs. In 2015, 53% of summer days are classified as HD_{L1}, while the other SSs show an average of 43% of HD_{L1}, while in 2017, these two percentages are 50% and 40%, respectively (Table 2).

Regarding Heat Waves' occurrence (Table 3), the difference is more marked. In the first group of SSs, in 2015, an average of four $HW_{\mathbf{L1}}$ for the sampling site is recorded; on the contrary, in the other group of SSs, this mean frequency is 2.5. In 2017, the $HW_{\mathbf{L1}}$ frequencies were 4.3 and 3.4, respectively. Moreover, also the Heat Waves intensity (or length of HWs) was significantly different: in 2015, for the first group of SSs, 73% of sampling days classified as HD_{L1}, which includes Heat Waves; on the contrary, in the other group of SSs, this percentage is 53%; in 2017, analogous behavior was observed, and the two percentage were 62% and 55%, respectively.

In the following, we present and discuss the results for the sampling site SS3 Badia (Parma, West Plain Area); this choice is based on the results previously discussed. SS3 shows a certain number of HW and HD that is statistically significant, allowing a detailed discussion of the correlation structure.

Using the HD and HW identification procedure [3], we introduce, as explained in Section 2.3, two external variables with double modalities (HD/noHD) and (HW/noHW) determining the submatrices:

$$(M_{HD})^{y}_{SS3} = [m_{HD}\ x\ n] \text{ and } (M_{noHD})^{y}_{SS3} = [m_{noHD}\ x\ n\ ]$$

$$(M_{HW})^{y}_{SS3} = [m_{HW}\ x\ n] \text{ and } (M_{noHW})^{y}_{SS3} = [m_{noHW} x\ 6\ DS].$$

in which n is the number of DS ($n = 6$); m_{HD} is the number of Hot Days; and m_{HW} is the number of Hot Days included in HW (reported in Table 5 as N number of sampling days). In Table 5, for each year and for each pollutant, we report the mean value calculated in summer and the percentage difference of mean values calculated only on sampling days classified as HD or HW. Levels of gaseous pollutants NO_x and O_3 show limited variations; on the contrary, the levels of particulate (PM_{10} and $PM_{2.5}$) show a significant increase in the HD and in the HW sampling day subsets. The concentration percentage increase is in the range 15–31%.

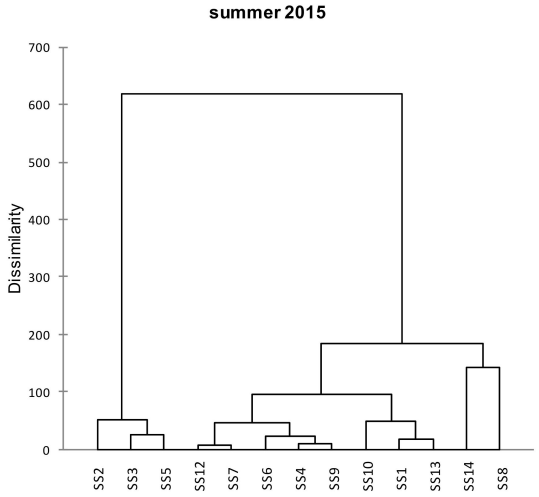

Figure 2. *Cont.*

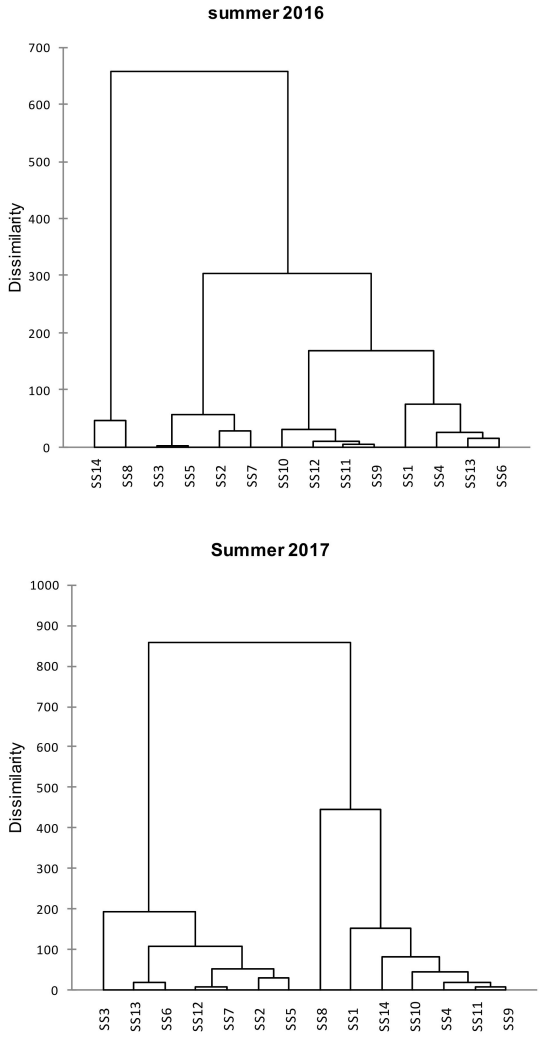

Figure 2. Dendrograms of sampling sites.

Table 5. Mean values (m_{tot} expressed in $\mu g/m^3$) of pollutants concentrations measured in SS3 sampling site and the corresponding percentage variation (Δm%) calculated with respect to mean values in Hot Days submatrices $(M_{HD})^{y}_{SS3}$ and to mean values in Heat Waves submatrices $(M_{HW})^{y}_{SS3}$ (N, number of sampling days).

	N	$m_{\text{tot}}(PM_{10})$	$m_{\text{tot}}(PM_{2.5})$	$m_{\text{tot}}(NO_x)$	$m_{\text{tot}}(O_3)$
M^{2015}_{SS3}	92	21	12.9	6.6	104.4
		Δm%	Δm%	Δm%	Δm%
$(M_{HD})^{2015}_{SS3}$	59	17%	16%	−3%	12%
$(M_{HW})^{2015}_{SS3}$	43	22%	22%	−4%	14%
	N	$m_{\text{tot}}(PM_{10})$	$m_{\text{tot}}(PM_{2.5})$	$m_{\text{tot}}(NO_x)$	$m_{\text{tot}}(O_3)$
M^{2016}_{SS3}	92	16.1	9.3	7.2	90.8
		Δm%	Δm%	Δm%	Δm%
$(M_{HD})^{2016}_{SS3}$	36	21%	18%	1%	18%
$(M_{HW})^{2016}_{SS3}$	13	31%	30%	−11%	14%
	N	$m_{\text{tot}}(PM_{10})$	$m_{\text{tot}}(PM_{2.5})$	$m_{\text{tot}}(NO_x)$	$m_{\text{tot}}(O_3)$
M^{2017}_{SS3}	92	18.1	9.6	6.6	106.5
		Δm%	Δm%	Δm%	Δm%
$(M_{HD})^{2017}_{SS3}$	53	17%	15%	6%	6%
$(M_{HW})^{2017}_{SS3}$	38	20%	17%	7%	8%

In last step, we applied PCA to submatrices $(M_{HD})^{y}_{SS3}$ and $(M_{noHD})^{y}_{SS3}$ (the submatrices $(M_{HW})^{y}_{SS3}$ and $(M_{noHW})^{y}_{SS3}$ are a subset of the previous matrices, and we obtained similar results). For the entire investigated period 2015–2017, in $(M_{HD})^{y}_{SS3}$, the first three factors explain more than 80% of data variance (Table 6), and the first factor is characterized by PM concentrations, whereas for $(M_{noHD})^{y}_{SS3}$ submatrices (Table 7), all the examined pollutants and meteorological parameters have a similar weight (about 20%) in the first factor, confirming the dominant role of particulate during Hot Days independent from relative humidity, which often plays an isolated role in the correlation structure. These results are comparable with what is described in Athene, where a worsening of the air-quality index is described in correspondence with HDs and HWs [19]. In our case, the pollutants that most increase their concentration in correspondence with heat waves are PM_{10} and $PM_{2.5}$.

Table 6. PCA results for HDs detected in SS3 sampling site. In the upper part of the table, the percentage of explained variance ($P\%$) and the cumulative percentage ($P_{cum}\%$) for the first three Principal Components (PC); in the lower part, the percentage weights ($w\%$) of the original descriptors in the new factors.

2015	***PC1***	***PC2***	***PC3***
$P\%$	56.0	26.4	8.1
$P_{cum}\%$		82.4	90.5
$w(PM_{10})\%$	26.2	0.3	12.1
$w(PM_{2.5})\%$	24.9	1.1	12.0
$w(NO_x)\%$	14.9	9.7	66.3
$w(O_3)\%$	22.9	0.6	45.2
$w(T_{max})\%$	10.9	34.2	0.1
$w(RH_{min})\%$	0.1	54.0	7.9
2016	***PC1***	***PC2***	***PC3***
$P\%$	45.0	26.2	14.7
$P_{cum}\%$		71.2	85.9
$w(PM_{10})\%$	29.3	1.7	9.0
$w(PM_{2.5})\%$	30.7	0.6	6.5
$w(NO_x)\%$	8.9	10.9	57.0
$w(O_3)\%$	12.1	19.6	23.3
$w(T_{max})\%$	0.6	56.1	0.1
$w(RH_{min})\%$	18.3	11.1	4.1
2017	***PC1***	***PC2***	***PC3***
$P\%$	41.8	23.7	18.0
$P_{cum}\%$		65.5	83.5
$w(PM_{10})\%$	33.6	3.4	0.4
$w(PM_{2.5})\%$	29.5	3.4	3.8
$w(NO_x)\%$	8.0	20.5	21.1
$w(O_3)\%$	5.1	5.9	56.0
$w(T_{max})\%$	21.9	15.1	8.3
$w(RH_{min})\%$	1.9	51.7	10.3

Our method allowed us to study the behavior of pollutants during extreme temperature events even if the concentrations of pollutants were not particularly high, while generally in the literature, we find comparisons between extreme events of concentration of pollutants and extreme events of temperature [23]. Moreover, our statistical procedure allowed us to make hypothesis also without a large database and on a local scale.

Table 7. PCA results for noHDs detected in SS3 sampling site. In the upper part of the table, the percentage of explained variance ($P\%$) and the cumulative percentage ($P_{cum}\%$) for the first three Principal Components (PC); in the lower part, the percentage weights ($w\%$) of the original descriptors in the new factors.

2015	***PC1***	***PC2***	***PC3***
$P\%$	50.7	28.5	10.6
$P_{cum}\%$		79.2	89.9
$w(PM_{10})\%$	28.8	3.4	0.2
$w(PM_{2.5})\%$	21.2	10.9	8.1
$w(NO_x)\%$	9.6	21.0	45.8
$w(O_3)\%$	18.7	9.3	22.8
$w(T_{max})\%$	19.6	13.8	3.5
$w(RH_{min})\%$	2.2	41.5	19.6
2016	*PC1*	*PC2*	*PC3*
$P\%$	48.6	26.2	12.3
$P_{cum}\%$		74.8	87.1
$w(PM_{10})\%$	21.0	18.6	2.1
$w(PM_{2.5})\%$	18.0	15.9	11.0
$w(NO_x)\%$	12.6	0.8	82.6
$w(O_3)\%$	20.7	11.1	3.9
$w(T_{max})\%$	24.8	6.6	0.1
$w(RH_{min})\%$	3.0	47.0	0.3
2017	*PC1*	*PC2*	*PC3*
$P\%$	48.4	27.1	11.5
$P_{cum}\%$		75.5	87.0
$w(PM_{10})\%$	26.3	6.5	1.7
$w(PM_{2.5})\%$	25.7	3.9	1.3
$w(NO_x)\%$	11.9	5.9	79.2
$w(O_3)\%$	12.4	24.6	16.0
$w(T_{max})\%$	9.2	31.8	1.8
$w(RH_{min})\%$	14.4	27.2	0.1

4. Conclusions

In this study, we present a statistical procedure investigating the behavior of air pollutants concentrations during Hot Day and Heat Waves. Our procedure was based on the following steps: definition of HD and HW from the comparison with the 30-year reference periods of each sampling site; identification of homogenous subgroups of sampling sites by means of Cluster analysis; and characterization of the correlation patterns among air pollutants during Hot Days and Heat Waves by means of Principal Component Analysis.

For the examined test case, by analyzing extreme events of maximum temperature through the identification of the number of occurrences of the Hot Days and their persistence (Heat Waves), it is possible to state that: summer 2016 presented a lower frequency of extreme event occurrence than summers 2015 and 2017; during the investigated and in examined area, no Heat Wave of the third level was identified. The last step of our procedure shows that there is a different behavior of pollutants during Heat Waves; particularly, Particulate Matter concentrations are higher independent from humidity, whereas NO_2 and O_3 concentrations seem to be not influenced by Heat Waves.

We want to emphasize that our procedure is easily applicable also in different geographical areas and with different pollutants. This method works well even if the pollutants' concentrations are low and if there are no large differences in the level of pollutants between Hot Days and no Hot Days.

The discussed procedure can be used in other contexts at local scale; it is useful for understanding the influence of extreme events on air pollutant concentrations and may be used by decision makers that have the responsibility of taking additional measures to prevent health effects on the population.

Author Contributions: Conceptualization, M.R., M.D., and V.T.; data curation, M.R. and L.C.; formal analysis, M.R.; investigation, M.R., M.D., L.C., and V.T.; methodology, M.R., M.D., and V.T.; resources, M.R., M.D., L.C., and V.T.; validation, M.R. and L.C.; writing—original draft, M.R. and M.D.; writing—review and editing, M.R. and M.D. All authors have read and agreed to the published version of the manuscript.

Funding: This research was funded in the framework of the project 'OT4CLIMA', which was funded by the Italian Ministry of Education, University, and Research (D.D. 2261 del 6.9.2018, PON R&I 2014–2020 and FSC.

Data Availability Statement: All analyzed data are freely downloaded from www.arpae.it. (accessed on 1 July 2021)

Conflicts of Interest: The authors declare no conflict of interest.

Abbreviations

ARPAE	Regional Agency for Prevention, Environment, and Energy of Emilia-Romagna
CA	Cluster Analysis
CLINO	CLImatological Normal
DS	Descriptor
HD	Hot Day
HW	Heat Wave
noHD	sampling day not classified as Hot Day
noHW	sampling day not included in an Heat Wave
PCA	Principal Component Analysis
PM	Particulate Matter
SS	Sampling Site
WMO	World Meteorological Organization

References

1. Battista, G.; de Lieto Vollaro, R. Correlation between air pollution and weather data in urban areas: Assessment of the city of Rome (Italy) as spatially and temporally independent regarding pollutants. *Atmos. Environ.* **2017**, *165*, 240–247. [CrossRef]
2. Kalisa, E.; Fadlallah, S.; Amani, M.; Nahayo, L.; Habiyaremye, G. Temperature and air pollution relationship during heatwaves in Birmingham, UK. *Sustain. Cities Soc.* **2018**, *43*, 111–120. [CrossRef]
3. Telesca, V.; Lay-Ekuakille, A.; Ragosta, M.; Giorgio, G.A.; Lumpungu, B. Effects on public health of heat waves to improve the urban quality of life. *Sustainability* **2018**, *10*, 1082. [CrossRef]
4. Cai, Z.; Tang, Y.; Chen, K.; Han, G. Assessing the Heat Vulnerability of Different Local Climate Zones in the Old Areas of a Chinese Megacity. *Sustainability* **2019**, *11*, 2032. [CrossRef]
5. Ebi, K.L.; Boyer, C.; Bowen, K.J.; Frumkin, H.; Hess, J. Monitoring and Evaluation Indicators for Climate Change-Related Health Impacts, Risks, Adaptation, and Resilience. *Int. J. Environ. Res. Public Health* **2018**, *15*, 1943. [CrossRef]
6. Dean, A.; Green, D. Climate change, air pollution and human health in Sydney, Australia: A review of the literature. *Environ. Res. Lett.* **2018**, *13*, 053003. [CrossRef]
7. Gallardo, L.; Barraza, F.; Ceballos, A.; Galleguillos, M.; Huneeus, N.; Lambert, F.; Ibarra, C.; Munizaga, M.; O'Ryan, R.; Osses, M.; et al. Evolution of air quality in Santiago: The role of mobility and lessons from the science-policy interface. *Elem. Sci. Anthr.* **2018**, *6*, 38. [CrossRef]
8. Dimitriou, K.; Kassomenos, P. The covariance of air quality conditions in six cities in Southern Germany—The role of meteorology. *Sci. Total Environ.* **2017**, *574*, 1611–1621. [CrossRef]
9. Mi, Z.; Guan, D.; Liu, Z.; Liu, J.; Viguié, V.; Fromer, N.; Wang, Y. Cities: The core of climate change mitigation. *J. Clean. Prod.* **2019**, *207*, 582–589. [CrossRef]
10. Demski, C.; Capstick, S.; Pidgeon, N.; Sposato, R.G.; Spence, A. Experience of extreme weather affects climate change mitigation and adaptation responses. *Clim. Chang.* **2017**, *140*, 149–164. [CrossRef] [PubMed]
11. Giorgio, G.A.; Ragosta, M.; Telesca, V. Climate variability and industrial-suburban heat environment in a Mediterranean area. *Sustainability* **2017**, *9*, 775. [CrossRef]
12. Elferchichi, A.; Giorgio, G.A.; Lamaddalena, N.; Ragosta, M.; Telesca, V. Variability of temperature and its impact on reference evapotranspiration: The test case of the Apulia Region (Southern Italy). *Sustainability* **2017**, *9*, 2337. [CrossRef]
13. Cioffi, F.; Conticello, F.; Lall, U.; Marotta, L.; Telesca, V. Large scale climate and rainfall seasonality in a Mediterranean Area: Insights from a non-homogeneous Markov model applied to the Agro-Pontino plain. *Hydrol. Process.* **2017**, *31*, 668–686. [CrossRef]
14. Yang, J.; Shao, M. Impacts of extreme air pollution meteorology on air quality in China. *J. Geophys. Res. Atmos.* **2021**, *126*, e2020JD033210. [CrossRef]

15. Hou, P.; Wu, S. Long-term Changes in Extreme Air Pollution Meteorology and the Implications for Air Quality. *Sci. Rep.* **2016**, *6*, 23792. [CrossRef]
16. Jorquera, H.; Villalobos, A.M.; Barraza, F. Ambient PM10 impacts brought by the extreme flooding event of 24–26 March 2015, in Copiapó, Chile. *Air Qual. Atmos. Health* **2018**, *11*, 341–351. [CrossRef]
17. Arbuthnott, K.G.; Hajat, S. The health effects of hotter summers and heat waves in the population of the United Kingdom: A review of the evidence. *Environ. Health* **2017**, *16*, 119. [CrossRef]
18. Zittis, G.; Hadjinicolaou, P.; Fnais, M.; Lelieveld, J. Projected changes in heat wave characteristics in the eastern Mediterranean and the Middle East. *Reg. Environ. Chang.* **2016**, *16*, 1863–1876. [CrossRef]
19. Papanastasiu, D.K.; Melas, D.; Kambezidis, H.D. Heat Waves characteristics and their relation to air quality in Athens. *Glob. Nest J.* **2014**, *16*, 919–928.
20. Lin, L.; Ge, E.; Liu, X.; Liao, W.; Luo, M. Urbanization effects on heat waves in Fujian Province, Southeast China. *Atmos. Res.* **2018**, *210*, 123–132. [CrossRef]
21. Katelaris, C.H. Climate Change and Extreme Weather Events in Australia Impact on Allergic Diseases. *Immunol. Allergy Clin.* **2021**, *41*, 53–62. [CrossRef]
22. Almeida, S.P.; Casimiro, E.; Calheiros, J. Effects of apparent temperature on daily mortality in Lisbon and Oporto, Portugal. *Environ. Health* **2010**, *9*, 12. [CrossRef]
23. Zhang, H.; Wang, Y.; Park, T.W.; Deng, Y. Quantifying the relationship between extreme air pollution events and extreme weather events. *Atmos. Res.* **2017**, *88*, 64–79. [CrossRef]
24. Mavrakis, A.; Kapsali, A.; Tsiros, I.X.; Pantavou, K. Air quality and meteorological patterns of an early spring heatwave event in an industrialized area of Attica, Greece. *Euro-Mediterr. J. Environ. Integr.* **2021**, *6*, 25. [CrossRef] [PubMed]
25. D'Amato, G.; Baena-Cagnani, C.E.; Cecchi, L.; Annesi-Maesano, I.; Nunes, C.; Ansotegui, I.; Canonica, W.G. Climate change, air pollution and extreme events leading to increasing prevalence of allergic respiratory diseases. *Multidiscip. Respir. Med.* **2013**, *8*, 12. [CrossRef]
26. De Sario, M.; Katsouyanni, K.; Michelozzi, P. Climate change, extreme weather events, air pollution and respiratory health in Europe. *Eur. Respir. J.* **2013**, *42*, 826–843. [CrossRef] [PubMed]
27. Gurney, K.R.; Romero-Lankao, P.; Seto, K.C.; Hutyra, L.R.; Duren, R.; Kennedy, C.; Pincetl, S. Climate change: Track urban emissions on a human scale. *Nat. News* **2015**, *525*, 179. [CrossRef]
28. Pandolfi, M.; Alastuey, A.; Pérez, N.; Reche, C.; Castro, I.; Shatalov, V.; Querol, X. Trends analysis of PM source contributions and chemical tracers in NE Spain during 2004–2014: A multi-exponential approach. *Atmos. Chem. Phys.* **2016**, *16*, 11787–11805. [CrossRef]
29. Arvani, B.; Pierce, R.B.; Lyapustin, A.I.; Wang, Y.; Ghermandi, G.; Teggi, S. Seasonal monitoring and estimation of regional aerosol distribution over Po valley, northern Italy, using a high-resolution MAIAC product. *Atmos. Environ.* **2016**, *141*, 106–121. [CrossRef]
30. Bigi, A.; Ghermandi, G. Trends and variability of atmospheric PM 2.5 and PM 10–2.5 concentration in the Po Valley, Italy. *Atmos. Chem. Phys.* **2016**, *16*, 15777–15788. [CrossRef]
31. Caserini, S.; Giani, P.; Cacciamani, C.; Ozgen, S.; Lonati, G. Influence of climate change on the frequency of daytime temperature inversions and stagnation events in the Po Valley: Historical trend and future projections. *Atmos. Res.* **2017**, *184*, 15–23. [CrossRef]
32. Field, C.B.; Barros, V.; Stocker, T.F.; Qin, D.; Dokken, D.; Ebi, K.L.; Mastrandrea, M.D.; Mach, K.J.; Plattner, G.K.; Allen, S.K. (Eds.) *Managing the Risks of Extreme Events and Disasters to Advance Climate Change Adaptation*; A Special Report of Working Groups I and II of the Intergovernmental Panel on Climate Change (IPCC); Cambridge University Press: Cambridge, UK, 2012; p. 582.
33. Beniston, M.; Stephenson, D.B.; Christensen, O.B.; Ferro, C.A.; Frei, C.; Goyette, S.; Halsnaes, K.; Holt, T.; Jylhä, K.; Koffi, B.; et al. Future extreme events in European climate: An exploration of regional climate model projections. *Clim. Chang.* **2007**, *81*, 71–95. [CrossRef]
34. Binaku, K.; Schmeling, M. Multivariate statistical analyses of air pollutants and meteorology in Chicago during summers 2010-2012. *Air Qual. Atmos. Health* **2017**, *10*, 1227–1236. [CrossRef]
35. Giorgio, G.A.; Ragosta, M.; Telesca, V. Application of a multivariate statistical index on series of weather measurements at local scale. *Measurement* **2017**, *112*, 61–66. [CrossRef]
36. Legendre, P.; Legendre, L. *Numerical Ecology*, 3rd ed.; Elsevier: Amsterdam, The Netherlands, 2012.
37. D.L. n.155 13/08/2010 Attuazione della Direttiva 2008/50/CE Relativa alla Qualità Dell'aria Ambiente e per un'aria più Pulita in Europa. Available online: https://www.camera.it/parlam/leggi/deleghe/10155dl.htm (accessed on 18 August 2021).